Research article

Synthesis and characterization of aluminum-yttrium perovskite powder via co-precipitation technique

Sara Ahmadi

Construction and Minerals Research Group, Technology and Engineering Research Center, Standard Research Institute, Alborz, Iran

A B S T R A C T

In this research the $YAlO_3$ perovskite powder (YAP) was successfully synthesized by co-precipitation route. Co-precipitation synthesis is simple and affordable technique that capable to produce more homogeneous powders. The temperature was lowered to 1400 °C as a result of the first step's investigation into how different mineralizers affect $YAlO_3$ formation. The next step involved examining the impact of pH on the synthesis process as well as the calcination time and temperature. The optimal conditions for the synthesis of single-phase YAP were subsequently determined. Scanning electron microscopy (SEM), inductively coupled plasma mass spectrometry (ICP-Mass), and X-ray diffraction (XRD) analysis have all been used to characterize the obtained powders. The findings demonstrate that the $NaF:MgF_2:Li_2CO_3$ (3:2:1 by weight) was the most suitable mineralizer system for formation of $YAlO_3$ perovskite. In addition, powders of orthorhombic YAP were successfully synthesized at pH=9. The optimal conditions for the preparation of single phase aluminum-yttrium perovskite crystals were found to be calcination at 1400 °C for 4 hours.

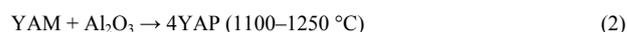## 1. Introduction

The Y_2O_3-Al_2O_3 system contains compounds with high technological impact, such as $YAlO_3$ orthorhombic perovskite (YAP), $Y_3Al_5O_{12}$ cubic garnet (YAG), and $Y_4Al_2O_9$ monoclinic yttrium aluminum oxide (YAM). YAP is recommended for cutting-edge applications such as laser and pigment host matrices, phosphor materials, scintillators, and thermoluminescent detectors due to its valuable features in pure phases and when doped with different rare earth elements. It is challenging to obtain single-phase YAP because YAG formation needs milder conditions and frequently exists as an impurity [1–3].

$YAlO_3$ is typically orthorhombic and has a perovskite (YAP) structure. The presence of a hexagonal modification (YAH) was also reported in some studies [4, 5]. Additionally, it is stated that while YAM and YAG are stable phases, YAP is semi-stable [3].

The ideal structure of perovskite with the formula of ABO_3 is a face-centered cubic (FCC) structure in which the B^{+3} cation with the smaller size is located in the octahedral spaces and has a neighborhood number of 12, while the larger A^{+3} ions are situated in the center of the unit cell. The phase transition in oxide systems is influenced by a number of variables, including raw materials, synthesis techniques, and thermal processes.

Several studies [5, 6] have reported the following sequence of Yttrium aluminates formation reactions with solid state reaction: the reaction between Al_2O_3 and Y_2O_3 proceeds through the diffusion of Al in Y_2O_3.

$$2Y_2O_3 + Al_2O_3 \rightarrow YAM\ (900\text{–}1100\ °C) \qquad (1)$$

$$YAM + Al_2O_3 \rightarrow 4YAP\ (1100\text{–}1250\ °C) \qquad (2)$$

$$3YAP + Al_2O_3 \rightarrow YAG\ (1400\text{–}1600\ °C) \qquad (3)$$

The phase transformation that occurs during the chemical synthesis method is very different from the one that occurs during the solid state route. Up to a temperature of 850 °C, co-precipitated powders of metal nitrates with a Y:Al molar ratio of 5:3 is amorphous. At 900 °C, hexagonal YAP that contains only a small amount of YAG is stable. As the temperature rises, the amount of YAG increases up to 1000 °C, and at higher temperatures, it crystallizes as a single phase [5].

Sim et al. have synthesized YAG via co-precipitation of nitrates, alkoxide, and modified alkoxide. The phase obtained with various heat treatments is summarized in Table 1. In this table, hexagonal $YAlO_3$ is shown as YAH [4].

In another research, YAG was synthesized at 800 °C using the co-precipitation method without the formation of any intermediate phase [7].

The orthorhombic YAP crystallization as $YAlO_3$ is complicated. Hess et al. demonstrated that the orthorhombic YAP crystallization in the glycine-nitrate process includes hexagonal YAP and YAM as intermediate phases. However, with long isothermal heat treatment at high temperatures (1500 °C and 24 hours), the sample contains orthorhombic YAP, and the amount of YAG and YAM is very low. Following is a summary of $YAlO_3$ crystallization [8]:

$$YAlO_3 \text{ amorphous} \rightarrow YAM \rightarrow YAH \rightarrow YAG \rightarrow \text{orthorhombic YAP} \quad (4)$$

In the other research, according to Ramanathan et al.'s report on the processing and characterization of combustion synthesized YAG powders, the as-formed precursor with $Y_3Al_5O_{12}$ stoichiometry heated up to 880 °C was amorphous. It underwent volatile loss and crystallization into YAP and YAG at 920 °C which transformed to pure YAG at 1050 °C [9].

Since 1960, aluminum yttrium garnet and perovskite have gained growing interest due to their remarkable optical applications in laser, microwave, and ultrasonic equipment.

Synthesis of YAP and YAG with solid state reactions requires high temperatures (1800 °C) and lengthy times [10, 11]. The main trend in recent years has been to concentrate on techniques for chemical synthesis like co-precipitation, sol-gel, and solution combustion [12–16]. With better homogeneity, greater level purity, and fewer stoichiometric losses, these synthesis techniques are very helpful in lowering the synthesis temperature. In comparison to other chemical methods, the co-precipitation technique is easier to use and requires less expensive raw materials and equipment [16]. Furthermore, it is reported that the mineralizers could reduce the synthesis temperature of YAP up to 1300 °C [17, 18]. However, luminescence properties decrease. In this study, a single-phase yttrium aluminum perovskite was synthesized through the co-precipitation procedure. The effect of pH, time, and temperature and also using the mineralizer was systematically investigated.

2. Experimental procedure

2.1. Starting materials and methods

Yttrium oxide (Y_2O_3, purity > 99.99%) and aluminum nitrate ($Al(NO_3)_3.9H_2O$, purity > 99.9%) were two of the reagent grade chemicals which were used in this study. Furthermore, NaF, MgF_2, KF, $BaCO_3$, and Li_2CO_3 were used as mineralizers [1, 2, 10, 11].

The $YAlO_3$ stoichiometry was followed in the preparation of the powders. Initially, a $Y(NO_3)_3$ solution was made by dissolving Y_2O_3 in diluted, hot nitric acid. A suitable quantity of aluminum nitrate aqueous solution was then added to the Yttrium nitrate solution. The resulting solution became unstable at a constant pH when 25% ammonia was gradually added.

The unstable solution was aged over the course of 24 hours by stirring. After filtering, distilled water was used to rinse the product. The finished product was dried at 100 °C for 24 hours. In an agate mortar, the specimens were made by combining the aforesaid powder with the chosen mineralizers. An electric furnace was used for heat treatment, which was done at various temperatures and times. The specimens were naturally cooled in the furnace after being heated at a rate of 10 °C/min. The flowchart of the described procedure is shown in Fig. 1.
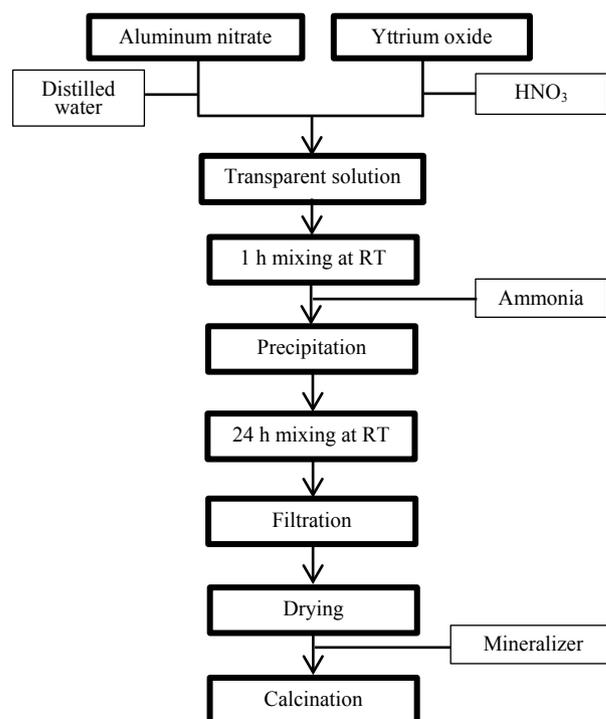

Fig. 1. Flow diagram of the chemical preparation procedure.

Table 1. The phases in aluminum-yttrium system synthesis via different raw materials [4].

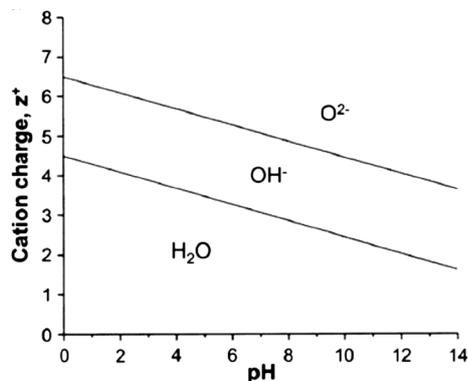| Temperature (°C)	Nitrate process	Alkoxide process	Modified alkoxide process
775	Amorphous phase	Amorphous phase	Amorphous phase
800	Amorphous + YAH + YAG	Amorphous phase + YAH	YAH + YAG
825	YAH + YAG	YAH	YAH + YAG
850	YAH + YAG	YAH	YAH + YAG
900	YAH + YAG	YAG + YAH	YAH + YAG
1000	YAG	YAG + YAM	YAG
1100	YAG	YAG	YAG + YAM

Fig. 2. Relationship among charge, pH, and cations equilibrium [21].

2.2. Characterization techniques

An XRD diffractometer (Simense, D500) equipped with a copper cathode was utilized to determine the crystallization behavior of the fired samples. The measurements were carried out in a 2θ range of 20–45 ° with a scan step of 0.02 ° and a time constant detection of 1 s in each step.

A scanning electron microscope (SEM: Stereoscan S360), equipped with an energy-dispersive X-ray spectrometer was used to analyze the morphology of synthetic powders. STA-1640 (PL-STA-1640) in the air was employed to perform simultaneous thermal analysis (STA). The heating rate was selected as 10 °C/min, and alumina powder was the reference material. The ICP analysis was used to investigate the number of cations in the washed water of precipitation.

3. Results and discussion

3.1. Effect of pH

The simultaneous precipitation of the cations is essential to maximum chemical homogeneity [19, 20], which can create ideal conditions for the formation of the YAlO$_3$ perovskite structure when using the co-precipitation method.
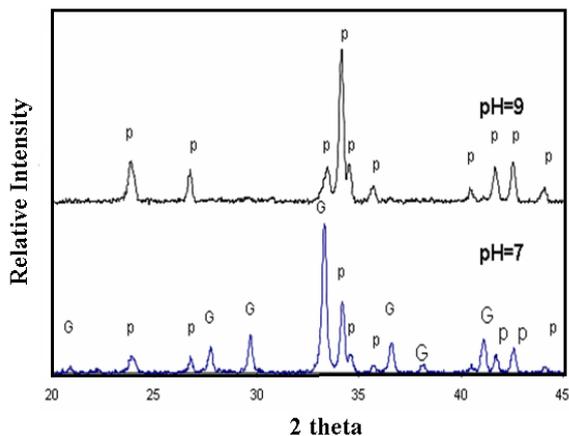

Fig. 3. XRD pattern of synthesized samples with different pH
(p: YAlO$_3$, G: Y$_3$Al$_2$(AlO$_4$)$_3$).

Table 2. Results of ICP analysis of washed water of precipitation.

| Element	Solution with pH 7	Solution with pH 9
Aluminum (ppm)	2047	0.66
Yttrium (ppm)	1253	0.08

In this method, with the increase of ammonia, the pH of the solution increases from the acidic state and system precipitate.

To investigate the effect of precipitation pH and complete hydrolysis of yttrium and aluminum and as a result to maintain stoichiometry, two samples were prepared with YAlO$_3$ composition with final pH of 7 and 9. After 24 hours of aging, the precipitations were washed with distilled water.

Table 2 shows the results of the ICP analysis of washed water of precipitation.

According to the table, although in the sample with pH 9, the amount of removed elements during washing is insignificant, the dissolved cations are removed during washing in the sample with pH 7. In the other words, this result confirms that pH 7 is not enough for the complete hydrolysis of the components of the YAlO$_3$.

Water molecules in an aqueous solution of Z^+-charged metal ions coordinate with the metal through electrons in their bonding orbitals. In turn, this causes the O-H bonds of bound water molecules to weaken and undergo protonation or hydrolysis depending on the pH (Eq. 5).

$$[M(OH_2)]^{z+} \rightarrow [M{-}OH]^{(z-1)+} + H^+ \rightarrow [M{=}O]^{(z-2)+} + 2H^+ \tag{5}$$
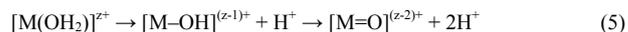
The high rate of hydrolysis for highly reactive metals may call for regulating water content and using nonaqueous solvents. Basic

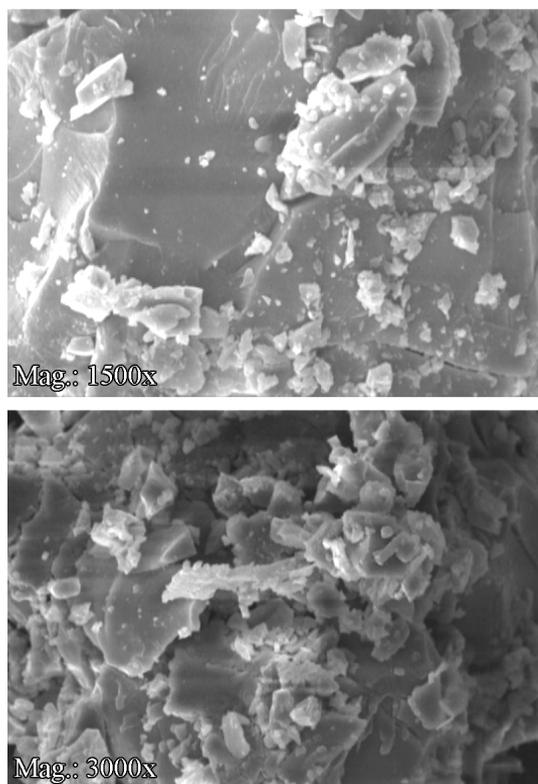**Fig. 4.** SEM images of dried precipitated powder.

Table 3. Composition and melting point of the samples.

Sample code	M1	M2	M3	M4	M5	M6	M7	M8
Composition (weight ratio)	KF	NaF	MgF_2	Li_2CO_3	KF:NaF (1:0.66)	KF:MgF_2 (1:5)	NaF:MgF_2 (1:5)	NaF:MgF_2:Li_2CO_3:(3:2:1)
Melting point (°C)	850	990	1270	720	710	778	835	-

conditions can shift the equilibrium to the right and favor the oxo ligands formation, while acidic conditions increase the ligands formation of hydroxo or even stop hydrolysis. In the case of less reactive metals, where an aqueous solution can be easily attained, the hydrolysis extent can be easily controlled by pH. Besides pH, cations of highly charged metal also tend to weaken the O–H bond and permit hydrolysis in bound water. In Fig. 2, the relation among hydrolysis equilibrium, pH, and charge is depicted [21].

Fig. 3 displays the XRD pattern of the dried precipitation following 2 h calcination at 1400 °C. It was observed that in the sample synthesized with pH 7, $Y_3Al_2(AlO_4)_3$ (cubic) phase is the main phase of the system, and the perovskite phase is present as a single phase in the sample synthesized with pH 9.

The scanning electron microscope (SEM) image of the dried powder obtained with pH 9 is shown in Fig. 4. It is evident that the powder is composed of relatively coarse agglomerates.

3.2. Effect of mineralizer

The perovskite structure development without mineralizer necessitates treatment of long isothermal at elevated temperatures, frequently exceeding 1800 °C. Therefore, utilizing an appropriate mineralizer system to accelerate the reactions is strongly recommended. The melting points of the mineralizer systems used in this research are shown in Table 3.

Fig. 5 depicts the XRD patterns of different mineralizers containing $YAlO_3$ specimens after 2 h of firing at the temperature of 1400 °C. In contrast to the M8 specimen that contains only perovskite, the remaining specimens include an unfavorable phase of cubic $Y_3Al_5O_{12}$. Precipitation of perovskite can only take place at 1400 °C.

Perovskite can only precipitate at 1400 °C by crystallizing from a liquid phase. Hence, it seems that a liquid phase is provided by the

mineralizers. Such a liquid phase can promote the diffusion rate of pigment ingredients within the initial steps of the heating process, enhance the growth of favorable crystals of $YAlO_3$, and decrease the temperature of synthesis.

The viscosity and quantity of this liquid phase have a significant impact on this procedure. Because of its low melting temperature (990 °C), sodium fluoride is easily evaporated and escapes from the system. In contrast, the MgF_2 that has a higher melting point (1270 °C) slowly evaporates. In the phase diagram, the M5-M7 mineralizer system that corresponds to the eutectic points of KF-NaF, KF-MgF_2, has a low melting temperature in the range of 710, 778, and 835 °C. Due to their high viscosity, they were ineffective as a mineralizer. It appears that adding Li_2CO_3 to the NaF-MgF_2 binary mineralizer system can reduce the system's melting point and viscosity due to the high field strength and small size of Li ions. However, with a ternary mineralizer system, the processes of dissolution and precipitation from the liquid phase are accelerated and lead to perovskite structure development. As a result, the mineralizer 3% NaF-2% MgF_2-1% Li_2CO_3 (wt%) was chosen as the system of interest in this research.

Fig. 5 depicts the XRD patterns of the fired samples with $YAlO_3$-based composition and the added mineralizers. As can be seen in Fig. 5, the only crystalline phase identified in the sample is once again perovskite. It means that the chosen composition has been appropriate to form the perovskite structure. Other researchers have obtained similar results using different mineralizers [11, 22].

3.3. Calcination temperature

The STA thermograph of the dried powder with 6 wt% of M8 mineralizer is shown in Fig. 6. It can be observed that up to 600 °C, the precipitation of hydroxides has turned into oxide, which is associated with a 40% weight loss. The weight loss in the TG diagram in this temperature range is related to the release of absorbed water, the release of crystalline water, the decomposition of nitrates, and the decomposition of hydroxides. The exothermic peak of crystallization is also observed at the temperature of 1000 °C.
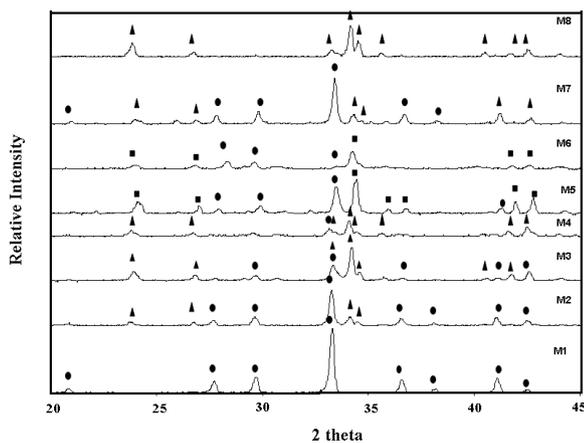

Fig. 5. XRD patterns of samples synthesized with different mineralizers mineralizers (▲ $YAlO_3$,● $Y_3Al_2(AlO_4)_3$, ■ $Y_3Al_5O_{12}$).
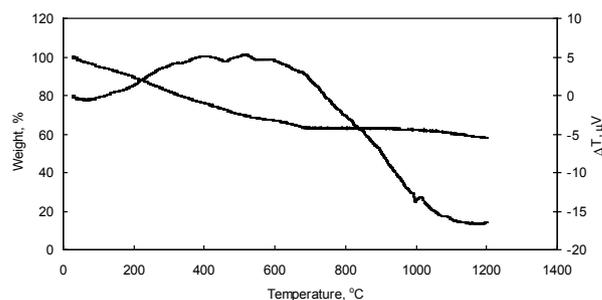

Fig. 6. STA traces of the dried precipitated powder at a rate of 10 °C/min.
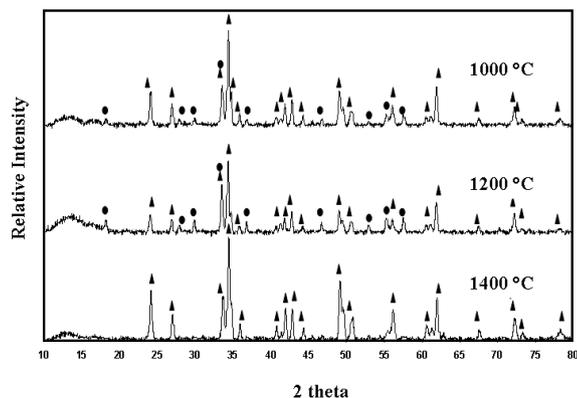
Fig. 7. XRD pattern of $YAlO_3$ powder, after calcination at different temperatures for 2 h ($\blacktriangle YAlO_3$, $\bullet Y_3Al_2(AlO_4)_3$).

The dried powders were calcined at 1000, 1200, and 1400 °C for 2 h to evaluate the phase development with temperature. Fig. 7 demonstrates the XRD patterns of mineralizers containing $YAlO_3$ after firing in various temperatures. As can be observed in Fig. 7, perovskite was the sole crystalline phase after calcination at 1400 °C, whereas the other firing temperature demonstrates an undesirable $Y_3Al_2(AlO_4)_3$ phase. It indicates that the heat treatment of co-precipitated powder at 1400 °C is suitable for the formation of the perovskite structure in the Al_2O_3-Y_2O_3 system. In other words, compared to solid state synthesis, the temperature required to form a perovskite structure using the co-precipitation method is significantly lower.

3.4. Calcination time

The XRD patterns of mineralizer containing $YAlO_3$ powder after firing at 1400 °C for 1, 2, and 4 h are depicted in Fig. 8. As it is seen in Fig. 8, after calcination for 2 h, $Y_3Al_5O_{12}$ and $Y_3Al_2(AlO_4)_3$ phases had disappeared from the sample. Increasing the soaking time of heating up to 4 h, did not change the crystallized phase. Therefore, the firing at 1400 °C for 2 h was chosen as the optimal calcination condition for the synthesis of $YAlO_3$ as a sole phase.

The powder's morphology and EDX analysis are shown in Fig. 9a and b, respectively. It is evident that the synthesized powder has both fine
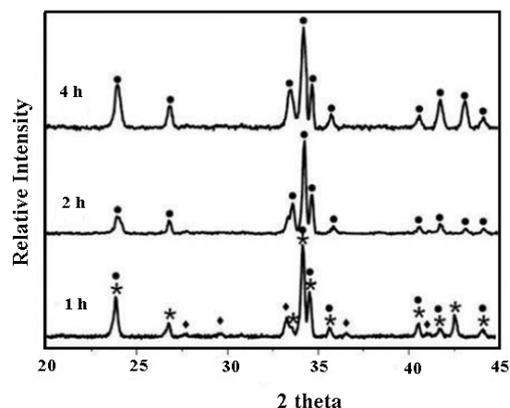

Fig. 8. XRD patterns of $YAlO_3$ powder, after calcination at 1400 °C for different time ($\bullet YAlO_3$, $\blacklozenge Y_3Al_2(AlO_4)_3$, $* Y_3Al_5O_{12}$).
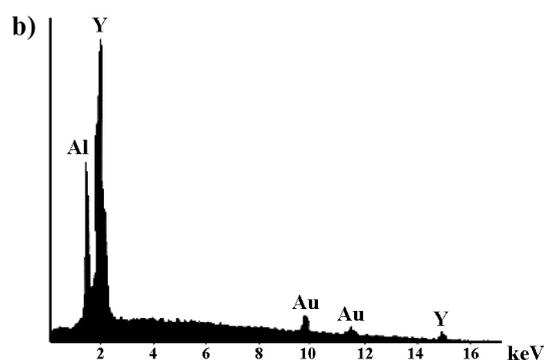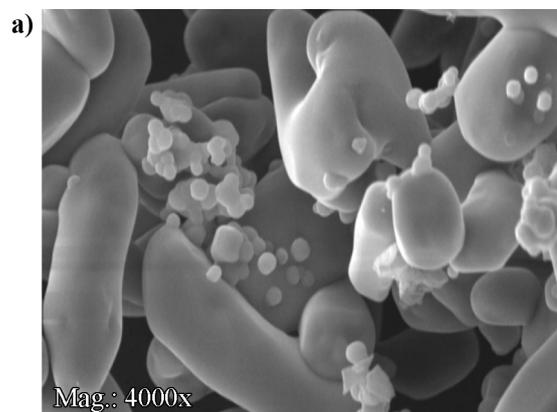

Fig. 9. a) SEM micrograph and b) the corresponding EDX analysis of $YAlO_3$ powder after calcination at 1400 °C for 2 h.

and coarse particles, a broad particle size distribution, and a morphology that resembles rods. Rod-shaped morphology resulted from dissolution and precipitation processes during crystallization. The SEM images thus support the mineralizer effect result that has been discussed. The homogeneity of the synthesized powder without any impurities is demonstrated by the elemental analysis by EDX. The fact that the perovskite phase formed as a single phase shows that both the conditions chosen for the synthesis and the co-precipitation method were effective in producing $YAlO_3$ with a perovskite structure.

4. Conclusions

The results of this research can be summed up as follows:

- $YAlO_3$ powder based on perovskite structure was successfully synthesized as a single phase via co-precipitation technique at a temperature lower than the solid state method.
- The pH of the solution in the co-precipitation method is an important factor in preventing of stoichiometric losses phase formation.
- Investigation of the effect of different mineralizers, including; NaF; KF; MgF_2; Li_2CO_3; KF:NaF (1:0.666); KF:MgF_2 (1:5); NaF:MgF_2 (1:5) and NaF:MgF_2:Li_2CO_3 (3:2:1) showed that NaF:MgF_2:Li_2CO_3 mineralizer has the most suitable effect in the formation of perovskite.
- Co-precipitation synthesis approach is an appropriate, simple, and relatively low-cost method for the synthesis of $YAlO_3$ structure. The high homogeneity in this method made it possible to achieve $YAlO_3$ perovskite as a single phase at 1400 °C for 2 h.

CRediT authorship contribution statement

Data availability

The data underlying this article will be shared on reasonable request to the corresponding author.

Declaration of competing interest

The author declares no competing interests.

Funding and acknowledgment

References

[1] R. Ianoş, R. Lazau, S. Borcanescu, R. Babut, Single-step combustion synthesis of YAlO3 powders, J. Mater. Sci. 50 (2015) 6382–6387. https://doi.org/10.1007/s10853-015-9190-y.

[2] E.M. Levin, C.R. Robbins, H.F. Mcmurdie, Phase diagrams for ceramists, The American Ceramic Society. (1964).

[3] Z. Shen, Å. Ekstrand, M. Nygren, Oxide/Oxide composites in the system Cr2O3-Y2O3-Al2O3, J. Eur. Ceram. Soc. 20 (2000) 625–630. https://doi.org/10.1016/S0955-2219(99)00261-7.

[4] S.M. Sim, K.A. Keller, T.-I. Mah, Phase formation in yttrium aluminum garnet powders synthesized by chemical methods, J. Mater. Sci. 35 (2000) 713–717. https://doi.org/10.1023/A:1004709401795.

[5] Y. Wang, L. Zhang, Y. Fan, J. Luo, D.E. McCready, et al., Synthesis, Characterization, and Optical Properties of Pristine and Doped Yttrium Aluminum Garnet Nanopowders, J. Am. Ceram. Soc. 88 (2005) 284–286. https://doi.org/10.1111/j.1551-2916.2005.00071.x.

[6] Y. Liu, L. Gao, Low-Temperature Synthesis of Nanocrystalline Yttrium Aluminum Garnet Powder Using Triethanolamine, J. Am. Ceram. Soc. 86 (2003) 1651–1653. https://doi.org/10.1111/j.1151-2916.2003.tb03535.x.

[7] J. Su, Q.L. Zhang, C.J. Gu, D.L. Sun, Z.B. Wang, et al., Preparation and characterization of Y3Al5O12 (YAG) nano powder by co-precipitation method, Mater. Res. Bull. 40 (2005) 1279–1285. https://doi.org/10.1016/j.materresbull.2005.04.009.

[8] N.J. Hess, G.D. Maupin, L.A. Chick, D.S. Sunberg, D.E. McCreedy, T.R. Armstrong, Synthesis and Crystallization of Yttrium Aluminium garnet & related compounds, J. Mater. Sci. 29 (1994) 1873–1878. https://doi.org/10.1007/BF00351307.

[9] S. Ramanathan, M.B. Kakade, S.K. Roy, K.K. Kutty, Processing and characterization of combustion synthesized YAG powders, Ceram. Int. 29 (2003) 477–484. https://doi.org/10.1016/S0272-8842(02)00190-6.

[10] X. Guo, K. Sakurai, Formation of Yttrium Aluminium Perovskite Garnet by Mechanical Solid state reaction, Jpn. J. Appl. Phys. 39 (2000) 1230–1234. https://doi.org/10.1143/JJAP.39.1230.

[11] M. Shirpour, M.A. Faghihi Sani, A. Mirhabibi, Synthesis and study of a new class of red pigments based on perovskite YAlO3 structure, Ceram. Int. 33 (2007) 1427–1433. https://doi.org/10.1016/j.ceramint.2006.04.023.

[12] S. Ahmadi, A. Aghaei, B. Eftekhari Yekta, Effective parameters for synthesis of chromium doped YAlO3 red pigment, Pigment. Resin Technol. 44 (2015) 1–6. https://doi.org/10.1108/PRT-02-2014-0013.

[13] P.A. Tanner, P.-T. Law, K.L. Wong, L. Fu, Preformed sol-gel synthesis and characterization of YAlO3, J. Mater. Sci. 38 (2003) 4857–4861. https://doi.org/10.1023/B:JMSC.0000004405.52574.37.

[14] U.S. Schubert, N. Hüsing, Synthesis of Inorganic Materials, Wiley–VCH. (2000).

[15] X. Li, L. Qiang, J. Wang, S. Yang, Effect of process parameters on the synthesis of YAG nano- crystallites in supercritical solvent, J. Alloys Compd. 421 (2006) 298–302. https://doi.org/10.1016/j.jallcom.2005.11.027.

[16] G. Xia, S. Zhou, J. Zhang, S. Wang, J. Xu, Solution Combustion synthesis, structure and luminescence of Y3Al5O12 :Tb+3 Phosphors, J. Alloys Compd. 421 (2006) 294–297. https://doi.org/10.1016/j.jallcom.2005.11.032.

[17] S. Ahmadi, A. Aghaei, B. Eftekhari Yekta, Synthesis of Y(Al,Cr)O3 red pigments by co-precipitation method and their interactions with glazes, Ceram. Int. 35 (2009) 3485–3488. https://doi.org/10.1016/j.ceramint.2009.04.029.

[18] R.I. Lazău, C. Păcurariu, D. Becherescu, R. Ianoş, Ceramic pigments with chromium content from leather wastes, J. Eur. Ceram. Soc. 27 (2007) 1899–1903. https://doi.org/10.1016/j.jeurceramsoc.2006.04.078.

[19] C.-C. Hwang, T.-Y. Wu, Synthesis and characterization of nanocrystalline ZnO powders by a novel combustion synthesis method, Mater. Sci. Eng. 111 (2004) 197–206. https://doi.org/10.1016/j.mseb.2004.04.021.

[20] Z. Yue, W. Guo, J. Zhou, Z. Gui, L. Li, Synthesis of nanocrystalline ferrites by Sol-Gel combustion process: the influence of pH value of solution, J. Magn. Magn. Mater. 270 (2004) 216–223. https://doi.org/10.1016/j.jmmm.2003.08.025.

[21] A.E. Danks, S.R. Hall, Z. Schnepp, The evolution of 'sol–gel' chemistry as a technique for materials synthesis, Mater. Horiz. 3 (2016) 91–112. https://doi.org/10.1039/C5MH00260E.

[22] Y. Marinova, J.M. Hohemberger, E. Cordoncillo, P. Escribano, J.B Carda, Study of solid solutions, with perovskite structure, for application in the field of ceramic pigments, J. Eur. Ceram. Soc. 23 (2003) 213–220. https://doi.org/10.1016/S0955-2219(02)00182-6.